

This paper is published as part of a *CrystEngComm* themed issue entitled:

Molecular Solids at Extreme Pressure

Guest Editors: Simon Parsons and Stephen Moggach
University of Edinburgh, UK

Published in [issue 9, 2010](#) of *CrystEngComm*

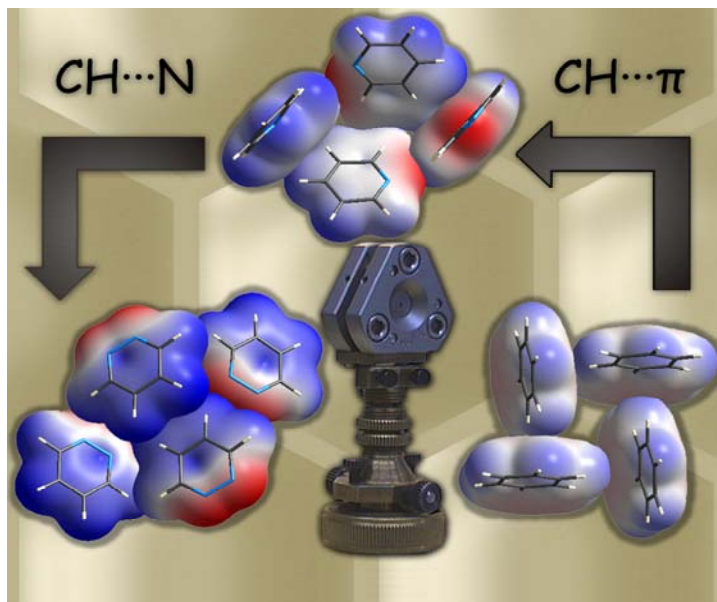


Image reproduced with permission Andrzej Katrusiak

Other articles published in this issue include:

[Pressure-induced switching in a copper\(II\) citrate dimer](#)

Kyle W. Galloway, Stephen A. Moggach, Pascal Parois, Alistair R. Lennie, John E. Warren, Euan K. Brechin, Robert D. Peacock, Rafael Valiente, Jesús González, Fernando Rodríguez, Simon Parsons and Mark Murrie, *CrystEngComm*, 2010, DOI: 10.1039/c001376e

[Density, freezing and molecular aggregation in pyridazine, pyridine and benzene](#)

Marcin Podsiadło, Katarzyna Jakóbek and Andrzej Katrusiak, *CrystEngComm*, 2010, DOI: 10.1039/c001153c

[Low temperature/high pressure polymorphism in DL-cysteine](#)

Vasily S. Minkov, Nikolay A. Tumanov, Raul Quesada Cabrera and Elena V. Boldyreva *CrystEngComm*, 2010, DOI: 10.1039/c003617j

[The effect of pressure on the crystal structure of L-alanine](#)

Nicholas P. Funnell, Alice Dawson, Duncan Francis, Alistair R. Lennie, William G. Marshall, Stephen A. Moggach, John E. Warren and Simon Parsons *CrystEngComm*, 2010, DOI: 10.1039/c001296c

Visit the *CrystEngComm* website for more cutting-edge crystal engineering research
www.rsc.org/crystengcomm

In situ investigations of the polyoxometalate Trojan Horse compound $K_7Na[W^{VI}_{18}O_{56}(SO_3)_2(H_2O)_2] \cdot 20H_2O$ under high temperature and high pressure conditions

Raúl Quesada Cabrera,^{ab} De-Liang Long,^c Leroy Cronin^{*c} and Paul F. McMillan^{*a}

Received 18th February 2010, Accepted 6th May 2010

DOI: 10.1039/c003388j

We have used Raman and IR spectroscopy to study the oxidation reaction of sulfite groups in the unique polyoxometalate compound $K_7Na[W^{VI}_{18}O_{56}(SO_3)_2(H_2O)_2] \cdot 20H_2O$ with a structure related to the Wells–Dawson type *in situ* at high temperature and high pressure. The results give new insights into the unusual redox process that occurs in this compound with electrons and O^{2-} ions transferred between the polyoxometalate cluster and SO_3^{2-}/SO_4^{2-} groups held within the cage in a process that has been termed the “Trojan Horse” effect.

1. Introduction

The polyoxometalates (POMs) are a large family of transition metal oxide cluster compounds formed by condensation of MO_n^{x-} units that are mainly tungstates, molybdates and vanadates. The well known Dawson structure type has general formula $[M_{18}O_{54}(XO_4)_2]^{m-}$ with $M = Mo$ or W and m achieving high values (up to 8–, depending on the metal oxidation state).¹ The POMs generally contain molecular anions XO_4^{x-} such as PO_4^{3-} , AsO_4^{3-} , or SO_4^{2-} within each $\{M_{18}\}$ cage. These compounds exhibit remarkable electronic properties and redox chemistry that are leading to applications in fields ranging from medicinal chemistry to photocatalysis.

Recent studies have concentrated on the unusual redox behaviour of POMs such as $K_7Na[W^{VI}_{18}O_{56}(SO_3)_2(H_2O)_2] \cdot 20H_2O$ that are related to the Dawson type. The structure of this compound has been described in detail elsewhere.² The cluster consists of two $[W_9(SO_3)]$ halves linked together through oxygen bridges by six equatorial tungsten atoms (Fig. 1). The SO_3 pyramids contained in the cluster are tilted, leaving four equatorial metal atoms uncoordinated and reducing the overall molecular symmetry to C_{2v} . Two of these four tungsten centres include a terminal water ligand that is released upon heating.² The proposed reaction for this observation involves the oxidation of the SO_3 groups inside the $[W_{18}]$ cage accompanied by rearrangement of the W–O bonding around the cluster and a colour change of the compound associated with partial reduction of the metal cluster shell (Scheme 1). This new redox process has been termed the “Trojan Horse” effect as a structural re-arrangement allows the two embedded pyramidal sulfite (SO_3^{2-}) anions to release up to four electrons (analogous to the “soldiers” hidden inside the “Trojan Horse”) to the surface of the cluster generating the sulfate-based, deep blue, mixed valence cluster $[W_{18}O_{54}(SO_4)_2]^{8-}$ (Scheme 1). In the present study, Raman

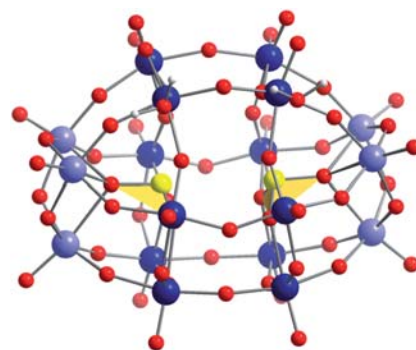
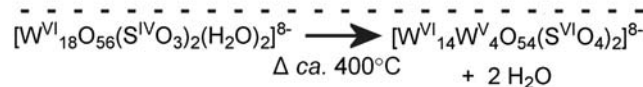


Fig. 1 Ball and stick representation of the C_{2v} symmetric “Trojan Horse” $[W_{18}O_{56}(SO_3)_2(H_2O)_2]^{8-}$ cluster anion (W: blue, O: red, H: grey, S: yellow). Yellow polyhedra represent the pyramidal SO_3 units and emphasize their orientation within the cage framework.



Scheme 1 This shows the proposed reaction within the “Trojan Horse” cluster at ambient pressure. A schematic is given above along with photographs of the starting and end material and a balanced reaction equation.

^aDepartment of Chemistry and Materials Chemistry Centre, Christopher Ingold Laboratories, University College London, London, WC1H 0AJ, UK. E-mail: p.f.mcmillan@ucl.ac.uk

^bSwiss-Norwegian Beam Lines, ESRF, Boite Postale 220, 38043 Grenoble, France

^cDepartment of Chemistry, The University of Glasgow, Glasgow, G128QQ, UK. E-mail: L.Cronin@chem.gla.ac.uk

and IR spectroscopy have been applied to study the temperature and pressure evolution of the title compound, while the pressure response has been monitored also by powder X-ray diffraction. Our results give new insights into the oxidation mechanisms of the SO_3^{2-} groups contained within the cluster and they also reveal the formation of bronze-like metal oxide species from POM structures under both high temperature and high pressure treatments.

2. Experimental

The sample of $\text{K}_7\text{Na}[\text{W}^{\text{VI}}_{18}\text{O}_{56}(\text{SO}_3)_2(\text{H}_2\text{O})_2] \cdot 20\text{H}_2\text{O}$ used in this study was synthesized using the procedure described previously.² For IR studies KBr pellets were prepared. The measurements were carried out using a Bruker IFS 66v/S spectrometer equipped with an IRscope II microscope and an LN₂-cooled MCT detector. Micro-Raman studies were performed on a Renishaw system with CCD detection and Mitutoyo 50 \times long-working distance objectives. Raman spectra were recorded throughout the sample using laser excitation wavelengths ranging from 477–780 nm minimising the incident power to minimise sample degradation. High-temperature studies were carried out at ambient temperature using a Linkam TS1200 stage. High-pressure studies were carried out using membrane or screw-driven diamond anvil cells (DACs) with type-IIa anvils, 600 μm culet-diameter for FTIR studies and type-Ia, 300 μm culet-diameter for Raman investigations. Stainless-steel gaskets were preindented to 40–50 μm thickness and holes of diameters 150–400 μm drilled by spark-erosion. Pressures were determined by ruby fluorescence. Synchrotron X-ray diffraction (XRD) studies were carried out at the Swiss-Norwegian Beam Lines at ESRF, BM01A using $\lambda = 0.7004 \text{ \AA}$ and MAR345 image plate as a detector. Two-dimensional diffraction data were analysed and converted to 1D patterns using Fit2D.³

3. Results

3.1. High-temperature IR spectroscopy results

The IR spectrum of the Trojan Horse compound at ambient conditions is in agreement with that reported earlier² (Fig. 2(a)). Following the analysis of the spectra developed for Keggin structures,⁴ the intense IR bands at 763, 817 and 918 cm^{-1} (Fig. 2(a)) could be assigned to W–O–W vibrations involving corner and edge-sharing oxygen atoms whereas the $\text{W}=\text{O}_t$ mode at 954 cm^{-1} involves terminal oxygen atoms. This band is usually considered as a pure stretching vibration in POM samples containing large organic counterions, where cluster–cluster interaction effects can be neglected. These assignments can only be regarded as tentative in the case of the POMs since (i) interactions between the metal oxide cages and the presence of charge balancing cations such as K^+ that bind strongly to the terminal and bridging oxo ligands can affect both the relative intensity and position of the IR bands and (ii) the modes are likely to have a combination of bending and stretching character. The broad bands at around 1630 and 3500 cm^{-1} are due to the bound H_2O molecules.

Upon heating to 150 $^\circ\text{C}$ (Fig. 2(b)), the sample colour changes from white to blue. The features due to bound (also solvated) water molecules disappear and these are replaced by H_2O vapour present in the sample chamber (the vibration–rotation features appear partly inverted because the interferogram was calibrated

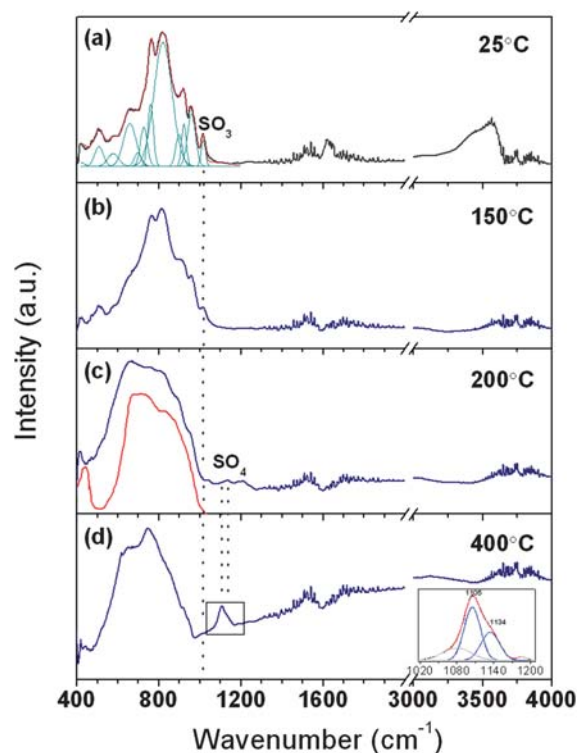


Fig. 2 IR spectra of the “Trojan Horse” compound during a heating run. The colour of the sample changes from white to blue at around 150 $^\circ\text{C}$. The red line in (c) corresponds to the IR spectrum of WO_3 reported in ref. 7. The inset in (d) shows the Gaussian fitting applied to the SO_4 bands emerging above 1100 cm^{-1} . The disappearance of the SO_3 mode and emerging of SO_4 bands are highlighted.

against a background obtained in water-free conditions). The vanishing of the bound water is consistent with the loss of the ligated H_2O from the cage upon oxidation of the sulfur atoms and reduction of the framework cage as shown in Scheme 1.

The bands become broadened at high temperature, especially upon heating to above 200 $^\circ\text{C}$ (Fig. 2(c)), although several vibrational features due to the cluster can still be identified. At 200 $^\circ\text{C}$, we clearly notice the vanishing of the mode at 1015 cm^{-1} that we assign to the $\nu_3(\text{S}-\text{O})$ stretching vibration of the SO_3 groups contained in the cluster. At the same time, we observe the appearance of weak broad bands between 1000 and 1200 cm^{-1} . Upon further heating, two of these bands, centred at 1108 and 1134 cm^{-1} , become more intense (Fig. 2(d)) and these correlate well with the reported assignment for $\nu(\text{S}-\text{O})$ stretching vibrations of SO_4 groups.⁵ The IR data are thus fully consistent with the redox reaction indicated in Scheme 1.

By 400 $^\circ\text{C}$ the spectral region associated with W–O vibrations is dominated by two broad bands centred around 748 and 649 cm^{-1} and there is a rising background to higher energy (Fig. 2(d)).

3.2. High-temperature Raman spectroscopy results

The Raman spectrum of the “Trojan Horse” compound at ambient conditions is dominated by a strong asymmetric peak at 980 cm^{-1} that can be fitted by two bands centred at 972 and 985 cm^{-1} , which correspond to asymmetric and symmetric

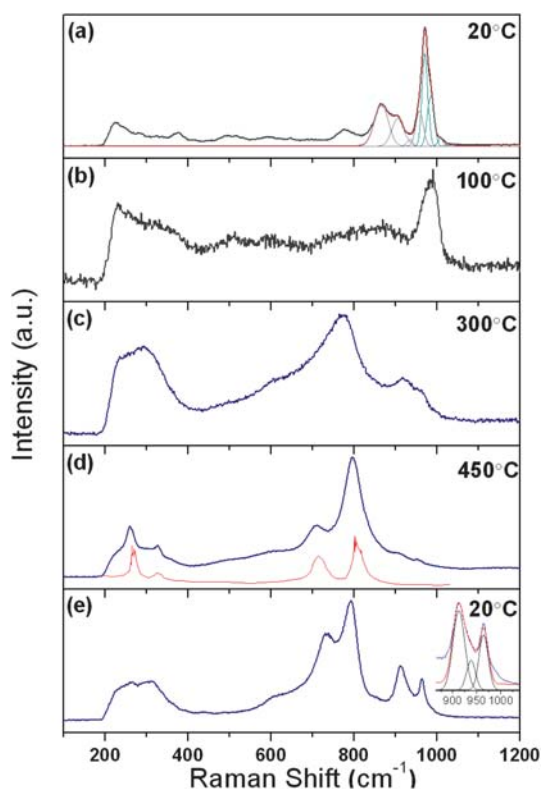


Fig. 3 Raman studies of $\text{K}_7\text{Na}[\text{W}^{VI}_{18}\text{O}_{56}(\text{SO}_3)_2(\text{H}_2\text{O})_2] \cdot 20\text{H}_2\text{O}$ upon heating. The spectrum of monoclinic WO_3 ⁷ is included in (d) for comparison (red line). (e) Raman spectrum of the recovered sample after the heating run. The inset reflects the Gaussian fitting of the intensified high-energy bands. The sample turned blue at around 200 °C.

$\nu(\text{W}-\text{O}_i)$ stretching modes involving terminal oxygen atoms⁴ (Fig. 3). On the high-energy side of this peak there is a broad low-intensity band at 1015 cm^{-1} that is assigned to $\nu_s(\text{S}-\text{O})$ stretching of the SO_3 anions in the structure as in the IR spectra. $\text{W}-\text{O}-\text{W}$ vibrations involving edge-sharing or corner-sharing oxygen atoms appear in the regions between 750 and 930 and 500 and 650 cm^{-1} , respectively. Most bands observed below 400 cm^{-1} are associated with $\text{W}-\text{O}$ stretching vibrations.

All of the bands broaden and their intensity diminishes dramatically upon heating to 100 °C (Fig. 3). The relative intensity decrease of the main peak is particularly marked and the vibrational features of the metal oxide structure are hardly recognisable at this temperature. By 200 °C the sample is blue and the Raman spectrum is dominated by a new broad band at 770 cm^{-1} and the peak at around 980 cm^{-1} is split into two components. These features are clearly observed in the spectrum at 300 °C (Fig. 3). A shoulder near 600 cm^{-1} is also observed.

Upon further heating to 450 °C, the new dominant 770 cm^{-1} becomes sharper and shifts up in frequency to 796 cm^{-1} together with the appearance of sharper peaks at 260, 327 and 709 cm^{-1} (Fig. 3).

The Raman spectrum obtained after recovery of the sample to ambient temperature shows a slight red shift of the main band to 790 cm^{-1} and a blue shift of the 709 cm^{-1} peak to 736 cm^{-1} (Fig. 3). There is also a relative intensity increase of the latter band. There is a marked sharpening and intensity increase in the two bands at 914 and 965 cm^{-1} . These changes observed in the Raman spectra

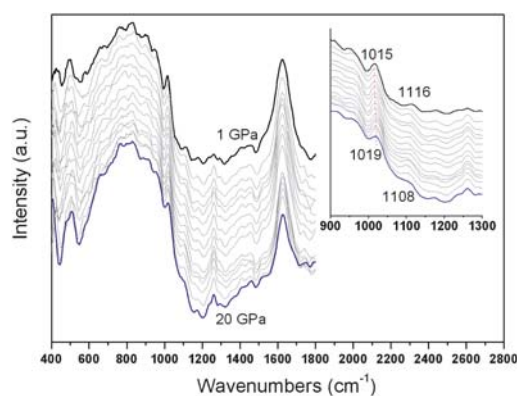


Fig. 4 High-pressure FTIR spectra of “Trojan Horse” compound upon compression up to 20 GPa. The inset highlights an apparent red shift of the band at 1116 cm^{-1} .

at high temperature will be discussed below, after presenting the results from *in situ* IR and Raman spectroscopy at high pressure.

3.3. High-pressure IR spectroscopy results

The IR bands from the metal oxide cage obtained under high-pressure conditions are broader than those observed in the high-temperature studies. Only a few changes were recorded in the spectra obtained up to 20 GPa, which was the maximum pressure attained in these studies (Fig. 4). A blue shift of most spectral bands is observed upon compression, as expected. However, the band at 1116 cm^{-1} shifts to 1108 cm^{-1} at 20 GPa (Fig. 4, inset). By analogy with the high-temperature IR studies, this could be related to the formation of SO_4 anions at high pressure, that would result in the appearance of a new band at 1108 cm^{-1} causing the apparent red shift of the one at 1116 cm^{-1} . That interpretation is supported by a decrease in the relative intensity of the 1015 cm^{-1} band due to the $\nu_s(\text{S}-\text{O})$ stretching mode of the SO_3^{2-} (Fig. 4). However, it is also possible that initiation of the oxidation process is being observed in these data taken at high pressure. It is interesting to note that, unlike the high-temperature investigation, bound water molecules remain within the POM during high-pressure studies, demonstrated by the persistence of the H_2O deformation peak at ~ 1630 cm^{-1} . The intensification of the doublet observed at 481 and 504 cm^{-1} with increasing pressure is discussed below.

3.4. High-pressure Raman spectroscopy results

The Raman spectra obtained at high pressure are shown in Fig. 5. The lowest pressure spectrum was obtained in the diamond anvil cell just after closure and the bands are slightly broadened compared with those recorded at ambient conditions previously (Fig. 3). Upon initial compression up to 13 GPa, the Raman peaks shift to higher energies and broaden further, except for the main $\text{W}=\text{O}_i$ band that exhibits a red shift to 992 cm^{-1} at 13 GPa (Fig. 5). The sample has become blue by 15 GPa and its Raman spectrum is much weaker. The $\text{W}=\text{O}_i$ band is observed at 985 cm^{-1} whereas the other features have become very broad. Only very broad bands can be observed at 24 GPa, with the most intense feature centred at 969 cm^{-1} (Fig. 5).

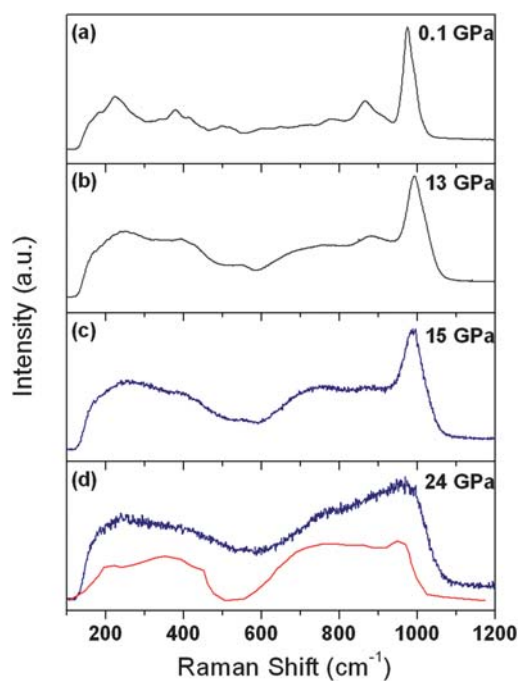


Fig. 5 Raman spectra of $\text{K}_7\text{Na}[\text{W}^{\text{VI}}_{18}\text{O}_{56}(\text{SO}_3)_2(\text{H}_2\text{O})_2] \cdot 20\text{H}_2\text{O}$ during compression up to 24 GPa. The spectrum of a $\text{M}_x\text{WO}_{3-y}$ film from the literature has been included for comparison ($\text{M} = \text{H}^+, \text{Li}^+$).⁶

3.5. High-pressure X-ray diffraction studies

We carried out preliminary synchrotron XRD studies in the DAC in order to examine pressure evolution of these POM compounds. Upon compression, a strongly textured powder pattern gradually evolves towards a simple hexagonal diffraction pattern (Fig. 6) along with the colour change of the sample from white to blue. Decompression does not change this hexagonal distribution of the diffracted intensity but it smears out the outer ring of previously broad Bragg spots. The sample remains blue

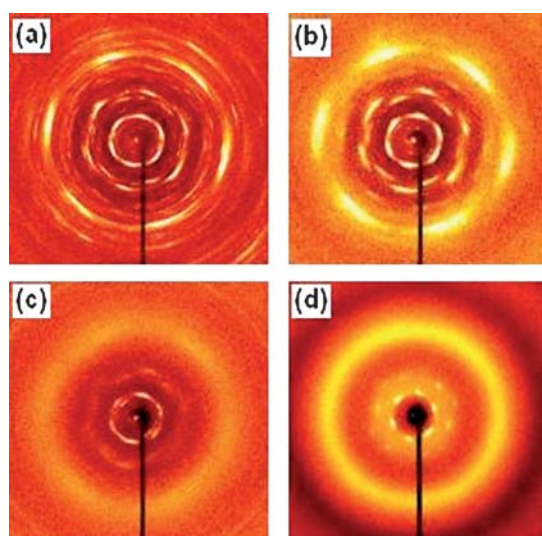


Fig. 6 Two dimensional XRD images recorded from the “Trojan Horse” POM compound during compression: (a) ambient pressure; (b) 14 GPa; (c) 21 GPa. Image (d) was taken during a scan of the material recovered to ambient conditions following the compression run.

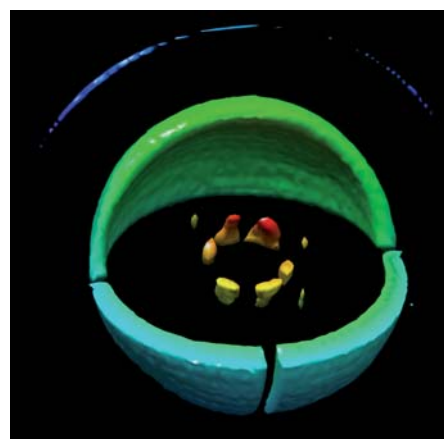


Fig. 7 Tomographic reconstruction of reciprocal space in rotation scanning of the blue sample at ambient conditions recovered following a compression run. The Bragg rods are identified in the centre of the image, together with spots of a secondary reflection. The outer shell results from the projection of the diffuse reflection surrounding the central Bragg features. The top blue arc is due to diffraction lines from the metal gasket.

upon recovery. This *in situ* diffraction experiment was complemented by *ex situ* rotation scan of the blue sample contained in the diamond cell gasket at ambient conditions following recovery after the compression run. This technique allows 3D reconstruction of reciprocal space (Fig. 7) and it has been widely used for mapping diffuse scattering and superstructure reflections; to the best of our knowledge it has not yet been applied to materials obtained from high-pressure studies. This 3D map shows that the first order reflections are in reality not Bragg spots but rods. In a simplest case of close packing of nearly spherical objects, this would correspond to a hexagonal structure with severe stacking disorder. Such a 2D structure, formed under pressure and then quenched to ambient conditions, could correspond to a structural disorder resulting in a dense packing of the metal oxide cluster groups in general agreement with spectroscopic data.

4. Discussion

The assignment of vibrational bands of large metal oxide clusters and the interpretation of their spectra upon changing experimental conditions are not trivial. This is especially the case for Wells–Dawson octadecatungstates, which have received little attention in the literature.⁷ However, the assignments summarised by Rocchiccioli *et al.*⁴ for Keggin ion units provide a useful starting point for understanding the behaviour of larger POM systems. These compounds are highly sensitive to light irradiation as indicated by their activity as photocatalysts, so that photoreduction and chemical decomposition of the clusters can occur during Raman spectroscopic studies and this must be taken into account during interpretation of the data.

The white-blue colour change observed during heating studies to above 150 °C occurs with no significant changes in the IR spectra, which points out to the ability of POM structures to accept electrons without major structural transformation.² The “Trojan Horse” redox reaction shown in Scheme 1 is confirmed

by the *in situ* high temperature IR data. In particular, the bands at 1108 and 1134 cm^{-1} indicating the presence of SO_4 anions⁵ identify the oxidation of the SO_3 groups, and bound H_2O is lost, confirming the redox reaction suggested previously.² The broadening of the cluster bands also indicates disordering occurring in the structure at high temperature and further disruption of the POM structure is evidenced upon additional heating (Fig. 2). The spectrum obtained at 200 °C shows broad features similar to WO_3 phases,⁸ and vibrational features appearing at higher temperatures resemble those observed for hydrated oxides⁹ or bronze-like species¹⁰ (Fig. 2).

In agreement with our IR results, changes in the Raman spectra taken at ambient pressure and high temperature between 200 and 300 °C suggest the formation of intermediate WO_3 phases within the sample⁸ (Fig. 3). Upon further heating there is a close resemblance between the POM spectrum and that reported for monoclinic WO_3 .⁸ The coexistence of this crystalline phase and an as yet unidentified amorphous modification is evidenced by the broad background in the spectrum.¹¹ Extra bands in the high energy region, that appear sharper and more intense following recovery of the sample to ambient conditions, indicate that the structural configuration deviates from that of the simple monoclinic WO_3 phase. These new bands could not be assigned unambiguously. However, similar bands have been observed in the formation of double $\text{W}^{\text{VI}}=\text{O}$ bonds involving terminal oxygen atoms, as previously identified in hydrated oxide species⁸ or amorphous tungsten oxide films.⁶ This situation could arise from the intercalation of K^+ and SO_4^{2-} ions in the metal oxide structure, as previously observed by intercalation of ions such as H^+ , Li^+ or Na^+ in WO_3 films.¹²

We expect that the materials derived from extreme compression treatment differ from those obtained at high temperature. In the case of WO_3 polymorphs we should expect the monoclinic phase containing small square channels to be more stable than the less dense hexagonal modification, which contains large channels in the structure. However, we must take into account the most stable structural model to accommodate water molecules and ions present in the “Trojan horse” structure, that cannot leave the system during the compression experiments at ambient temperature. Our high-pressure IR spectra contain intense bands at 481 and 504 cm^{-1} that are common to hydrated hexagonal WO_3 phases reported by Daniel *et al.*⁸

A red shift of the $\text{W}-\text{O}_i$ band related to the reduction of W^{VI} atoms has been reported in the Raman investigation of the transformation of WO_3 into H_xWO_3 bronzes.¹³ The formation of bronze-like species also correlates with the broad bands appearing around 300 and 800 cm^{-1} (Fig. 5) which closely resemble those reported by Mioc *et al.*¹⁰ The Raman spectrum shown at 24 GPa (Fig. 5) can be directly compared with spectra reported for amorphous M_xWO_3 films ($\text{M} = \text{H}^+$, Li^+ , *etc.*) upon increasing content of ions in a pure WO_3 film.⁶ These authors suggest that the insertion of electrons into the M_xWO_3 films reduce the W^{VI} to W^{V} species, as previously indicated for the “Trojan horse” POM compound.² The H^+ or Li^+ ions occupy interstitial positions without strong bonds with the metal oxide structure. Thus, the corresponding single $\text{W}^{\text{V}}-\text{O}$ and double $\text{W}^{\text{V}}=\text{O}$ bonds would be expected to occur at around 330 and 450 cm^{-1} , respectively,⁶ and the intensity of the $\text{W}^{\text{VI}}-\text{O}$ band would decrease in agreement with our Raman results upon compression (Fig. 5).

Although the same white-blue colour change as observed in the high-temperature experiments occurred in the high pressure sample beyond 15 GPa, the presence of SO_4 groups could not be confirmed from the Raman studies at high pressure (Fig. 5). This could result from a disordered arrangement of these anions within the structure, as observed in amorphous sulfate materials found at high pressure.¹⁴ The resulting compound at high pressure would consist of a layered $(\text{WO}_3)_{2n}-(\text{SO}_4)$ structure containing WO_6 octahedra with a small number of SO_4 tetrahedral groups randomly occupying interstitial positions. Analogous disordered bronze-like species have been proposed for the products obtained following high temperature treatment of other POM structures.¹⁰

5. Conclusions

The *in situ* IR experiments on $\text{K}_7\text{Na}[\text{W}^{\text{VI}}_{18}\text{O}_{56}(\text{SO}_3)_2(\text{H}_2\text{O})_2]$ at high temperature (up to 200 °C) confirm the “Trojan Horse” hypothesis for the unusual redox reaction scheme.² IR and Raman experiments on the POM sample during heating (over 200 °C) and compression studies also indicate the formation of tungsten oxide bronze-like species.

Acknowledgements

This study was supported by an EPSRC Senior Research Fellowship to PFM and a Royal Society & Wolfson Foundation Research Merit award to LC. We thank V. Dmitriev for access to the Swiss-Norwegian Beam Lines (ESRF) and D. Chernyshov and O. Leynaud (Institute Néel, CNRS) for contributions to the XRD analysis.

References

- 1 M. T. Pope, *Heteropoly and Isopoly Oxometalates*, Springer-Verlag, Berlin, 1983; D.-L. Long, R. Tsunashima and L. Cronin, *Angew. Chem., Int. Ed.*, 2010, **49**, 2.
- 2 D.-L. Long, H. Abbas, P. Kögerler and L. Cronin, *Angew. Chem., Int. Ed.*, 2005, **44**, 3415.
- 3 A. P. Hammersley, S. O. Svensson, M. Hanfland, A. N. Fitch and D. Häusermann, *High Pressure Res.*, 1996, **14**, 235.
- 4 C. Rocchiccioli-Deltcheff, M. Fournier, R. Franck and R. Thouvenot, *Inorg. Chem.*, 1983, **22**, 207; R. Thouvenot, M. Fournier, R. Franck and C. Rocchiccioli-Deltcheff, *Inorg. Chem.*, 1984, **23**, 598.
- 5 J.-F. Lemonnier, S. Floquet, J. Marrot and E. Cadot, *Eur. J. Inorg. Chem.*, 2009, 5233.
- 6 S.-H. Lee, H. M. Cheong, C. E. Tracy, A. Mascarenhas, D. K. Benson and S. K. Deb, *Electrochim. Acta*, 1999, **44**, 3111.
- 7 R. I. Buckley and R. J. H. Clark, *Coord. Chem. Rev.*, 1985, **65**, 167.
- 8 M. F. Daniel, B. Desbat and J. C. Lassegues, *J. Solid State Chem.*, 1987, **67**, 235; J. V. Gabrusenoks, P. D. Cikmach, A. R. Lusia, J. J. Kleperis and G. M. Ramans, *Solid State Ionics*, 1984, **14**, 25; M. F. Daniel, B. Desbat, J. C. Lassegues and R. Garie, *J. Solid State Chem.*, 1988, **73**, 127.
- 9 B. Pecquenard, H. Lecauchoux, J. Livage and C. Julien, *J. Solid State Chem.*, 1998, **135**, 159–168.
- 10 U. B. Mioc, R. Z. Dimitrijevic, M. Davidovic, Z. P. Nedic, M. M. Mitrovic and P. H. Colombari, *J. Mater. Sci.*, 1994, **29**, 3705.
- 11 Y. Shigesato, A. Murayama, T. Kamimori and K. Matsuhiro, *Appl. Surf. Sci.*, 1988, **33/34**, 804.
- 12 P. Delichere, P. Falaras, M. Froment and A. H.-L. Goff, *Thin Solid Films*, 1988, **161**, 35.
- 13 E. Cazzanelli, C. Vinegoni, G. Mariotto, A. Kuzmin and J. Purans, *Solid State Ionics*, 1999, **123**, 67.
- 14 A. K. Arora and T. Sakuntala, *Solid State Commun.*, 1990, **75**, 855.